INDIAN JOURNAL OF SCIENCE AND TECHNOLOGY

RESEARCH ARTICLE

🔓 OPEN ACCESS

* **Corresponding author**.

bezakiyya@gmail.com

Competing Interests: None

Comparative Analysis of Conventional (CDTC) and Torque Controller Output Manipulated Stator Flux Angle Based Direct Torque Control (TCSF-DTC) of Permanent Magnet Synchronous Motor (PMSM)

Berhanu Deggefa Lemma[1]*, **Srinivasan Pradabane**[1]

1 Department of Electrical Engineering, National Institute of Technology Warangal, India

Abstract

Objective: It is recommended to use DTC when a quick response time is required. However, the ripple in torque, as well as flux, is the biggest drawback of DTC. This study presents a comparative analysis of two direct torque control methods CDTC and TCSF-DTC for PMSM's that operate at a constant speed. **Method:** Matlab 2021b is used to model both CDTC and TCSF-DTC including all switching signals generation. During the simulation, the switching state is chosen to achieve a fast torque and flux response. **Finding:** A comparison of the two methods was made based on the results of the simulation. In comparison to CDTC, TCSF-DTC uses double-tracking control to manipulate flux values, which minimizes flux ripples. Although the torque performance is similar in both cases, TCSF-DTC has better flux ripple minimization. In both cases, the torque ripple is 2.857%, whereas the flux ripple is 1.879% and 0.1% for CDTC and TCSF-DTC respectively Furthermore, the simulation result for the supply voltage of the motor illustrates improvements in the harmonic distortion and fundamental component magnitudes. **Novelty**: Flux and torque are controlled independently in DTC, but a PI controller is added for TCSF-DTC. This study compares the performance of CDTC and TCSF-DTC for flux and torque ripple at a constant speed to recommend the control scheme that is suitable for fine torque and flux ripple control. It has been raised in several works that DTC ripples can be reduced, and researchers have recommended several DTC algorithms, including model-predictive DTC, space vector pulse width modulated DTC, and duty ratio optimization. As a result of adding this feature, computational complexity increases. In particular, duty ratio optimization increases computation complexity for slope estimation. The main advantage of this scheme is that it does not increase the complexity of signal processing but it is effective in minimizing flux ripple.

Keywords: Direct torque; flux angle; flux ripple; permanent magnet synchronous motor; torque ripple

1 Introduction

These days, many researchers are working diligently on controlling algorithms and motor design to enhance the performance of PMSM [1]. The reduction in computation time affects the response and performance of the total drive system by reducing the burden on the processor, as stated in [2]. Even though PMSM is designed for continuous duty operation, high efficiency, high power density, and compact design, it is susceptible to high torque ripples when a direct torque control algorithm is used. Ripple has a significant impact on the motor and supply components of PMSMs that operate at high temperatures and loads. According to [3–5] adding model parameters to a control algorithm and signal processing can improve the performance of a system due to the thermal effects. The PMSM motor parameter changes nonlinearly with temperature and loads current. It is proposed to include the nonlinear nature of a control system for PMSM in [6,7]. The influence of magnetic saturation on PMSM operation and performance has been studied in many research. Flux variation is very important when it comes to control and performance when using DTC. In [8], the effect of parameter variation on the operation performance of the permanent magnet synchronous motor (PMSM) is studied. According to [8], Motor performance figures like ripple torque, ripple current, and speed are highly influenced by parameter variation.

In drive applications where a fast response is required, direct torque control is recommended. Quick response in torque for PMSM is obtained by manipulating the angle quickly. Quick angle manipulation is achieved by omitting the null voltage level so that the angle can be varied. DTC controls torque and flux directly. In this way, DTC's field weakening capabilities are enhanced. It is proposed to implement direct torque control based on space vector (DTC-SVM) to minimize flux and torque ripple in [9]. The switching signal generation is achieved by using the space vector technique. Minimization of ripple in flux, torque, and the number of commutations using reference flux vector calculator, PI controller, and space vector modulation in the place of error in torque, error in flux, hysteresis controller, and switching table is explored in [9].

Space vector modulation-based direct torque control (DTC-SVM) is proposed as the control scheme which reduces the ripple for both torque and flux when it is seen from a generic DTC perspective. A direct torque control system, based on space vector pulse width modulation, is utilized in [10], to reduce ripple torque using the predictive current to estimate flux magnitude. DTC is composed of solely torque and flux control schemes. To further reduce flux ripple, the PI control and torque are used to manipulate the stator flux phase angle in TCSF-DTC. Flux variation and control play a big role in variable speed ranges and reducing ripple. A comparative analysis of CDTC and (TCSF-DTC) is presented in this work, focusing on torque ripple, flux ripple, at different loading conditions and for constant speed operation. DTC control has a good feature in terms of response. But the main drawback of DTC is a ripple which is the main concern of this study. On the aforementioned literature proposed, different algorithms were forwarded to minimize the ripple for both torque and flux. But even though, the aforementioned methods were effective in reducing torque it adds computation complexity. The proposed method is applied to the constant speed control of PMSM. Flux which has a direct link with speed needs to be controlled with high accuracy to obtain the constant flux with a less complex modified CDTC. So in this work, the TCSF-DTC is applied to control the PMSM, to have a minimum flux ripple with a simple algorithm. This work is organized into mathematical modeling, material and method, results and discussion, and a conclusion.

2 Mathematical modeling of PMSM

The mathematical model of PMSM is depicted by equations below:

$$V_q = R * i_q + \frac{d}{dt}(\psi_q) + \omega_s * \psi d \tag{1}$$

$$V_d = R * i_d + \frac{d}{dt}(\psi d) - \omega_s * \psi_q \tag{2}$$

$$\begin{cases} \psi sd = L_d * i_d + m_f \\ \psi sq = Lq^* i\, q \end{cases} \tag{3}$$

$$T_e = 3/2 * P_n * (mf^* i_q + (Ld - Lq)^* i\, q^* i\, d) \tag{4}$$

$$J * \frac{d}{dt}(\omega_r) = T_e - T_L - B^* \omega_r \tag{5}$$

$$\omega_s = \frac{p}{2} * \omega_r \tag{6}$$

$$\theta_r = \int \omega_s dt \tag{7}$$

$$i_q = \frac{1}{L_q} \int (V_q - R^* i_q - \omega_s * \psi_d)\, dt \tag{8}$$

$$i_d = \frac{1}{L_d} \int (V_d - R^* i_d + \omega_s * \psi q)\, dt \tag{9}$$

The coordinate transformation for dq-abc and $\alpha\beta$-dq is performed by equations (10) and (11) shown below respectively.

$$\begin{matrix} V_a \\ V_b \\ V_c \end{matrix} = \sqrt{\frac{2}{3}} * \begin{bmatrix} \cos(\theta r) & -\sin(\theta r) & \sqrt{1/2} \\ \cos(\theta r - 2/3 * pi) & -\sin(\theta r - 2/3 * pi) & \sqrt{1/2} \\ \cos(\theta r + 2/3 * pi) & -\sin co(\theta r + 2/3 * pi) & \sqrt{1/2} \end{bmatrix} * \begin{matrix} V_q \\ V_d \\ V_0 \end{matrix} \tag{10}$$

$$\begin{cases} \psi s\alpha \\ \psi s\beta \end{cases} = \begin{bmatrix} \cos(\theta r) & -\sin(\theta r) \\ \sin(\theta r) & \cos s(\theta r) \end{bmatrix} * \begin{matrix} \psi sd \\ \psi sq \end{matrix} \tag{11}$$

3 Materials and Methods

The PMSM model, inverter model, signal processing, and switching signal generation are done in a d-q axis using Matlab 2021b. During signal manipulation, flux and torque estimation are performed, which are used for signal generation. The voltage selection for CDTC and TCSF-DTC is executed in such a way that the applied voltage gives a fast response in monitoring flux and torque. According to the work stated in [6], for the n sector, a vector Vn+1 is used to increase both flux and torque. In contrast, Vn+5 is applied to decrease torque and increase flux. The voltage Vn+2 is used to rise torque and reduce flux whereas Vn+4 is employed to reduce both respectively. With TCSF-DTC, torque deviation and PI controllers are used to manipulate flux angle, to have further control over the flux.

According to the TCSF-DTC, the flux angle is calculated by adding the output of the torque controller and the flux angle calculated from the estimated flux.

$$\text{angle}_{flu\,x} = \text{angle}_{fhx} + \left(k_p + \frac{k_i}{s}\right) * (\text{Tref} - Te) \tag{12}$$

We can represent torque as a function of flux angle, which manipulates the flux mathematically. It is possible to have a positive or negative torque error.
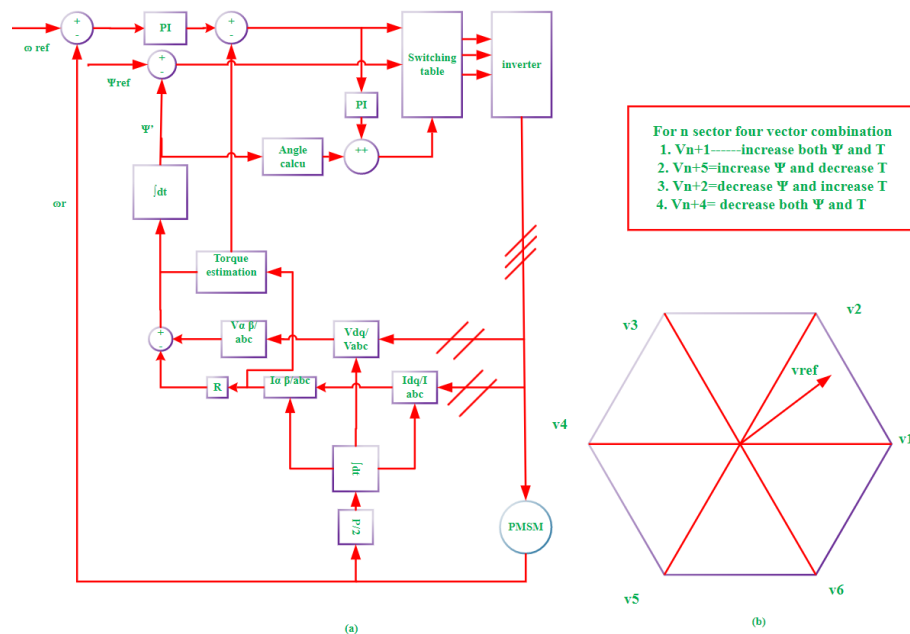
Fig 1. (a) shows a layout of TCSF-DTC, (b) shows the switching state for fast torque and flux response
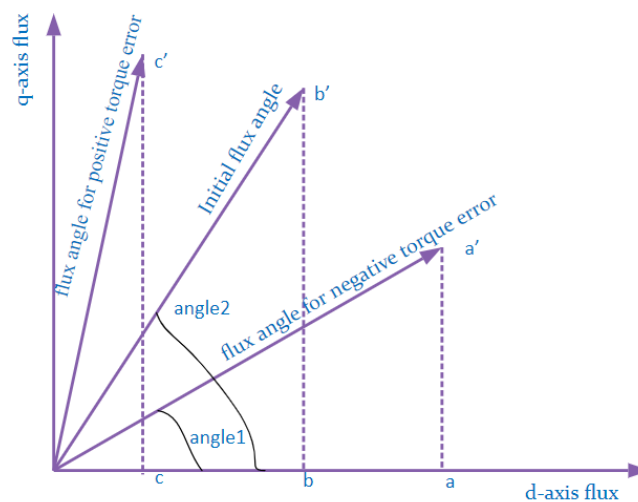

Fig 2. Shows the effect of torque error on the magnitude of the flux

When the reference torque differs from the electromagnetic torque, there is a torque error. Positive errors mean that the reference is greater than needed, and vice versa. The torque equation (4) shows that the quadrature current component and the d-axis flux are significant contributors to torque production. In particular, the quadrature current plays a crucial role. When the torque error is negative, the flux angle decreases, which decreases the flux on the q-axis. According to equation (3), q-axis flux depends on q-axis current. Figure 2 shows that if the original angle is angle2 and the torque error is negative, the angle of flux changes from angle2 to angle1. When the angle is angle2, the q-axis flux is at b', whereas when angle manipulation occurs, the angle is changed to angle1 and the magnitude of q-axis flux is changed to a'. A current quadrature component can be calculated based on this information.

Whereas the d-axis flux changes from b to a, according to the picture depicted in Figure 2. The change of the q-axis current is negative which means the current should reduce bring back the error to zero. So according to this relation, the torque flux angle manipulation is applied in this work to change the magnitude of flux based on torque error. This could enhance, the flux

ability to track the reference torque.

$$\Delta i\, q = \frac{b' - a'}{Lq} \tag{13}$$

4 Result and discussion

4.1 Result for CDTC

Fig 3. For the graph on the left, (a) shows the torque when red indicates the reference torque and blue indicates developed torque, (b) shows the speed when red indicates the reference speed and blue indicates motor speed, (c) shows the current magnitude, (d), (e), (f) shows the three-phase voltage magnitude, for the graph on the right, (a) shows the d-axis flux, (b) shows the q-axis flux, (c) shows the magnitude of flux with ripple, and (d) shows the plot of flux.
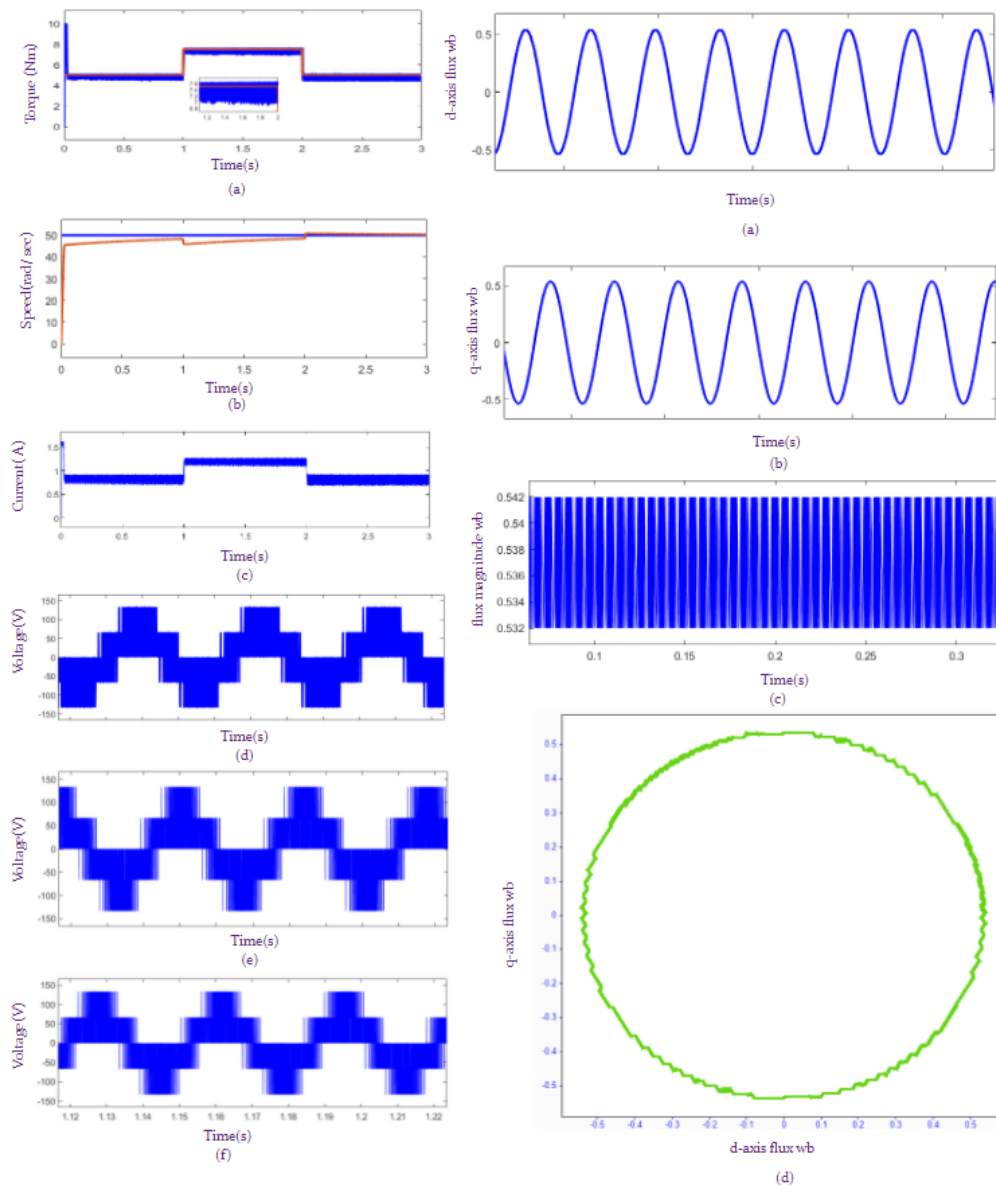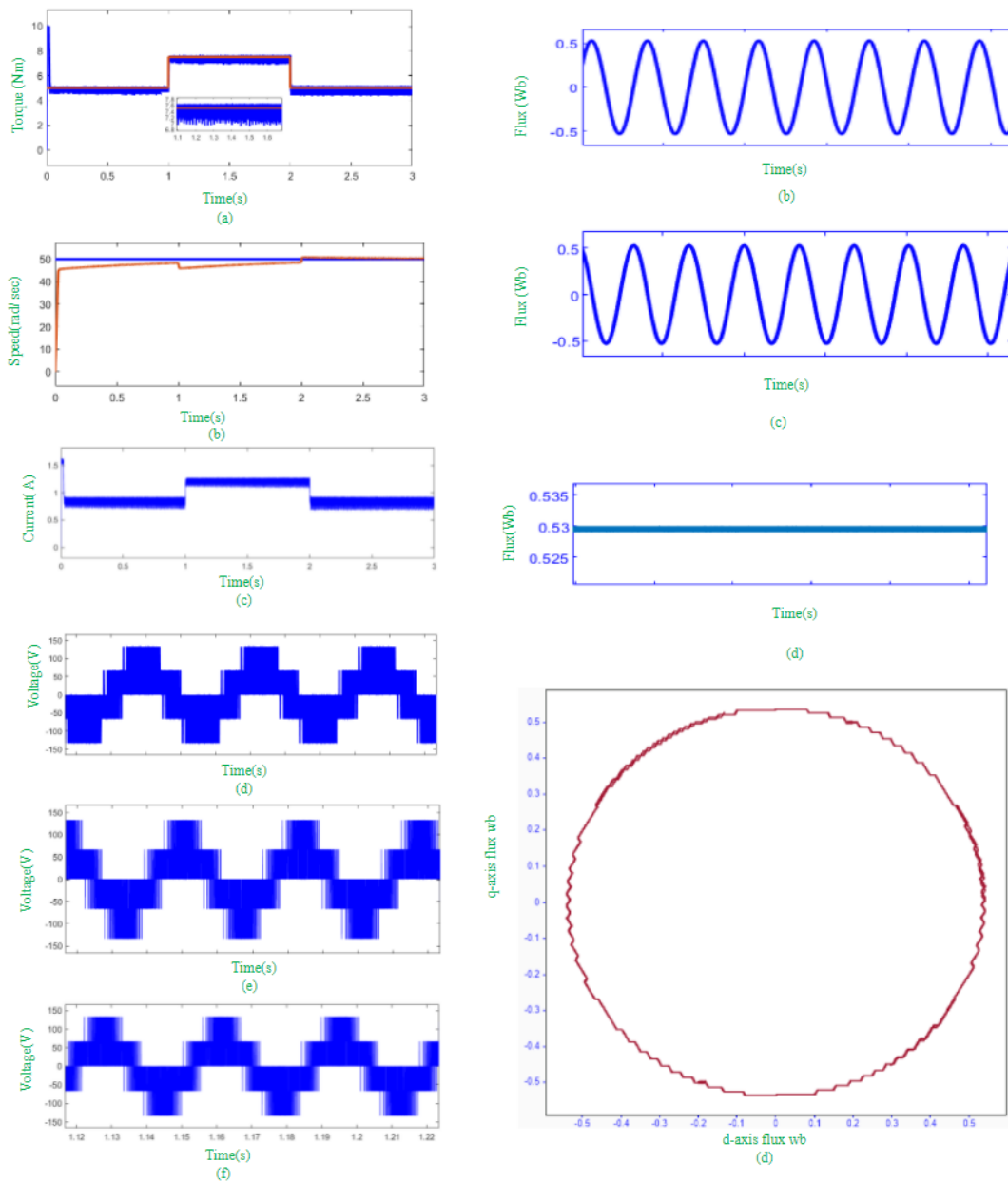
4.2 Result for TCSF-DTC

Fig 4. For the graph on the left, (a) shows the torque when red indicates the reference torque and blue indicates developed torque, (b) shows the speed when red indicates the reference speed and blue indicates motor speed, (c) shows the current magnitude, (d), (e), (f) shows the three-phase voltage magnitude, for the graph on the right, (a) shows the d-axis flux, (b) shows the q-axis flux, (c) shows the magnitude of flux with ripple, and (d) shows the plot of flux.
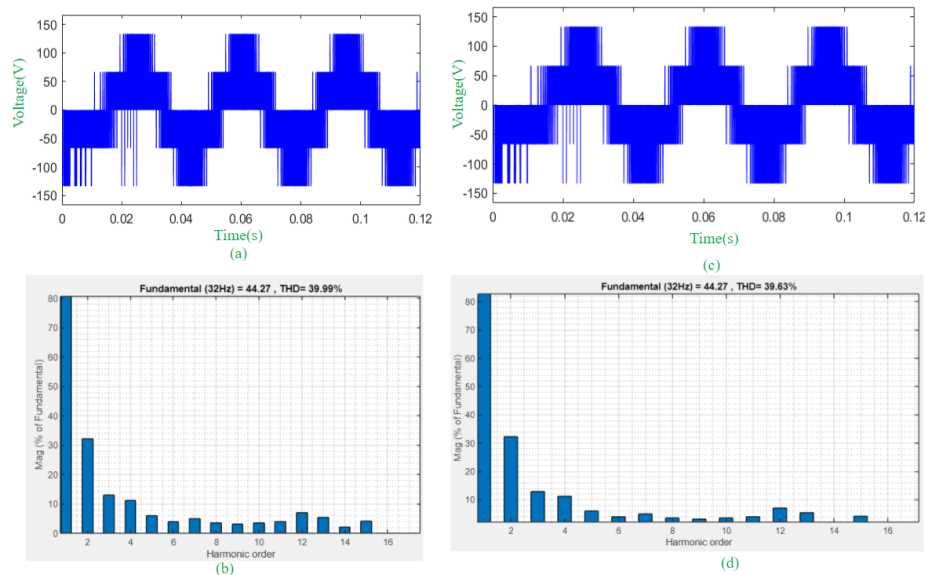
Fig 5. (a) shows the voltage waveform for CDTC, (b) shows the voltage harmonic component and total harmonic distortion for CDTC, (c) shows the voltage for TCSF-DTC, (d) shows the harmonic component and total harmonic distortion for TCSF-DTC.

Table 1. Motor parameter and data used for simulation

Parameter	Magnitude	Parameter	Magnitude	Parameter	Magnitude	Parameter	Magnitude
Ld	21.3mH	Bm	0.001	Lq	24.2mH	Tl	10 Nm
fs	500hz	Ra	0.24 ohm	mf	0.542wb	ω	50 rad/sec
Im	10A	P	8	J	0.0024	Vdc	200V

5 Discussion

The simulation is conducted at a constant speed. The torque was made to change at the magnitude of half of the rated torque, seventy-five percent of the rated torque, and half of the rated torque respectively, and these detachment times are 0 to 1 second, 1 to 2 seconds, and 2 to 3 seconds respectively. Compared to CDTC, TCSF-DTC has one additional PI controller as is shown in figure 1. The PI controller is used to further manipulate the flux angle. Due to this double manipulation on flux, the flux ripple reduction of TCSF-CDTC is better than CDTC. The torque ripple control components are the same for both cases. In addition to the double manipulation of flux magnitude using both PI controller and conventional DTC regulation, the voltage selection is based on the error reduction strategy. So the effect of enhanced voltage selection and double manipulation of flux makes the system have a better performance. In the simulation, the switching state is selected according to the methodology shown in figure 1(b). Simulated outcomes of both the CDTC and TCSF-DTC methods were obtained at a constant speed. Due to TCSF-DTC's double control manipulation on flux values, ripples on flux are minimized when TCSF-DTC is used compared to CDTC. In both cases, the torque performance is similar as shown in Figure 3(a) and Figure 4(a) on the right graph. The torque fluctuation remains between 7.0 and 7.6 for the reference torque of 7.5. On average, there is a ripple of 2.857%. According to figure 3(c) on the left, the CDTC flux is between 0.532 and 0.542 for a reference value of 0.532 and its ripple is 1.879%. However, in the case of TCSF-DTC, the flux remains in the range of 0.525 to 0.535, as shown in figure 4(c) on the left. Flux ripple for this control method is 0.1%. So the torque performance of the CDTC and TCSF-DTC is similar whereas TCSF-DTC has better performance flux ripple minimization. From this work, it can be seen that CDTC is preferable for torque ripple reduction as the scheme has no computation for angle manipulation which is the case of TCSF-DTC. In addition, from the simulation result in Figure 5(b) and Figure 5(d), it can be seen that total harmonic distortion of motor input voltage is less when TCSF-DTC is used compared to CDTC.

6 Conclusion

This study presents two direct torque control methods for PMSM at constant speed operation. The two DTC applied for PMSM were compared in terms of torque ripple, flux ripple, and input voltage total harmonic distortion. Simulated outcomes of both the CDTC and TCSF-DTC methods were obtained at a constant speed. According to the simulation result of TCSF-DTC's, due to double control manipulation on flux values, ripples on flux are minimized when TCSF-DTC is used compared to CDTC. In both cases, the torque performance is similar. From this work, it can be seen that CDTC is preferable for torque ripple reduction as the scheme has no computation for angle manipulation which is the case of TCSF-DTC. As the fine control of an electric drive is the hot topic for a research area, an interested person can consider TCSF-DTC with a duty ratio optimization for a torque error minimization as TCSF-DTC has a superior flux ripple performance.

References

1) Bida VM, Samokhvalov DV, Al-Mahturi FS. PMSM vector control techniques — A survey. *2018 IEEE Conference of Russian Young Researchers in Electrical and Electronic Engineering (EIConRus)*. 2018;p. 577–581. doi:10.1109/EIConRus.2018.8317164.

2) Xia C, Liu N, Zhou Z, Yan Y, Shi T. Steady-State Performance Improvement for LQR-Based PMSM Drives. *IEEE Transactions on Power Electronics*. 2018;33(12):10622–10632. Available from: https://dx.doi.org/10.1109/tpel.2018.2803760. doi:10.1109/tpel.2018.2803760.

3) Li K, Wang Y. Maximum Torque per Ampere (MTPA) Control for IPMSM Drives Using Signal Injection and an MTPA Control Law. *IEEE Transactions on Industrial Informatics*. 2019;15(10):5588–5598. Available from: https://dx.doi.org/10.1109/tii.2019.2905929. doi:10.1109/tii.2019.2905929.

4) Jiang W, Feng S, Zhang Z, Zhang J, Zhang Z. Study of Efficiency Characteristics of Interior Permanent Magnet Synchronous Motors. *IEEE Transactions on Magnetics*. 2018;54(11):1–5. Available from: https://dx.doi.org/10.1109/tmag.2018.2847328. doi:10.1109/tmag.2018.2847328.

5) Wang Q, Yu H, Wang M, Qi X. An Improved Sliding Mode Control Using Disturbance Torque Observer for Permanent Magnet Synchronous Motor. *IEEE Access*. 2019;7:36691–36701. Available from: https://dx.doi.org/10.1109/access.2019.2903439. doi:10.1109/access.2019.2903439.

6) Wu X, Huang W, Lin X, Jiang W, Zhao Y, Zhu S. Direct Torque Control for Induction Motors Based on Minimum Voltage Vector Error. *IEEE Transactions on Industrial Electronics*. 2021;68(5):3794–3804. Available from: https://dx.doi.org/10.1109/tie.2020.2987283. doi:10.1109/tie.2020.2987283.

7) Xue Y, Yu H, Liu X. Improved Fuzzy Backstepping Position Tracking Control for Manipulator Driven by PMSM. *2018 Chinese Automation Congress (CAC)*. 2018;p. 3561–3565.

8) Lemma BD, Pradabane S. Control of Permanent-Magnet Synchronous Motors Using Fuzzy Logic Considering Parameter Variation and Diagnostic Capability For Hostile Environment Applications. *2020 IEEE First International Conference on Smart Technologies for Power, Energy and Control (STPEC)*. 2020;p. 1–4.

9) Nasr A, Gu C, Wang X, Buticchi G, Bozhko S, Gerada C. Torque-Performance Improvement for Direct Torque-Controlled PMSM Drives Based on Duty-Ratio Regulation. *IEEE Transactions on Power Electronics*. 2022;37(1):749–760. Available from: https://dx.doi.org/10.1109/tpel.2021.3093344. doi:10.1109/tpel.2021.3093344.

10) Lemma BD, Pradabane S. Ripple torque lessening in space vector pulse width modulation based direct torque control of permanent magnet synchronous motor drive. *Journal of Physics: Conference Series*. 2021;1817(1):012027–012027. Available from: https://dx.doi.org/10.1088/1742-6596/1817/1/012027. doi:10.1088/1742-6596/1817/1/012027.